Research Square

Preprints are preliminary reports that have not undergone peer review.
They should not be considered conclusive, used to inform clinical practice,
or referenced by the media as validated information.

Hydrogen sulfide donor GYY4137 protects against atherosclerosis by modulating autophagic activity

Lijun Luo
1. College of Pharmacy, North Sichuan Medical College

Qiuhong Dong
1. College of Pharmacy, North Sichuan Medical College

Rong Huang
1. College of Pharmacy, North Sichuan Medical College

Chunlei Yu
1. College of Pharmacy, North Sichuan Medical College

Chunyan Yang
1. College of Pharmacy, North Sichuan Medical College

Chunyang Zhou
zhouchunyang@nsmc.edu.cn

1. College of Pharmacy, North Sichuan Medical College

Research Article

Keywords: Atherosclerosis, GYY4137, Hydrogen sulfide, Autophagy

Posted Date: February 25th, 2026

DOI: https://doi.org/10.21203/rs.3.rs-8718130/v1

License: This work is licensed under a Creative Commons Attribution 4.0 International License.
Read Full License

Additional Declarations: No competing interests reported.

Abstract

Objective

Atherosclerosis (AS) constitutes the central pathological process underlying major cardiovascular ailments, such as coronary heart disease and myocardial infarction, and is a primary driver of global morbidity and premature mortality. Hydrogen sulfide (H_2S) confers protective effects on AS. The aim of this study is to explore the effect of hydrogen sulfide donor GYY4137 in atherosclerosis and its potential mechanism.

Methods

Macrophages were treated with ox-LDL to establish atherosclerosis models in *vitro*. Cell viability was assessed by Cell Counting Kit-8 (CCK-8). Total cholesterol (TC), free cholesterol (Fch), and cholesteryl ester (CE) were detected by cholesterol esterase assay. Lipid accumulation was measured by Oil Red O staining. The autophagy markers (LC3-II, p62) were tested by Western blotting.

Result

Ox-LDL induced foam cells formation and led to autophagy dysregulation, whereas GYY4137 alone exhibits no cytotoxicity or disruption of autophagy. Furthermore, GYY4137 can reduce the LC3 Ⅱ/LC3Ⅰ ratio of foam cells, as well as the expression of p62 protein.

Conclusion

GYY4137 has protective effects on ox-LDL induced macrophage foam cell, and this protective effect is related to the regulation of autophagy.

1. Introduction

Cardiovascular diseases (CVDs) remain the leading cause of global mortality. Most of these deaths were from heart attacks and strokes. These conditions are primarily caused by the progression of atherosclerosis and subsequent plaque rupture[1, 2]. Atherosclerosis, a chronic inflammatory condition of the arterial wall, involves the accumulation of lipids and fibrous components, which gives rise to plaque development and subsequent narrowing of the arterial lumen[3]. Histological studies have demonstrated oxidized low-density lipoprotein (ox-LDL) plays an important role in the pathophysiology of atherosclerosis by triggering inflammatory responses in vascular endothelial cells (VECs), smooth muscle cells (SMCs), and macrophages[4]. In this study, macrophages were treated with ox-LDL to establish atherosclerosis models in *vitro.*

Macroautophagy/autophagy is a highly conserved intracellular process that maintains cellular homeostasis by facilitating the lysosomal degradation of long-lived proteins and damaged organelles[5]. This process begins with the proteolytic cleavage and lipidation of LC3, wherein the cytosolic form (LC3-I) is converted to the autophagosome-membrane bound form (LC3-II)[6]. p62, as an autophagic substrate, can bind to the autophagic protein LC3 for consumption, leading to a reduction in autophagosomes[7]. Consequently, the LC3-II/LC3-I ratio, the protein level of LC3-II and p62 serves as the key biomarkers for evaluating autophagic activity. Critically, autophagy is a dynamic multi-step process. Disruption of autophagic flux at any stage leads to aberrant p62 accumulation. This, in turn, triggers inflammatory responses that exacerbate atherosclerosis (AS)[8]. Therefore, maintaining unimpeded autophagic flux presents a promising therapeutic strategy for AS protection.

Hydrogen sulfide (H_2S), recognized as the third gas transmitter after nitric oxide (NO) and carbon monoxide (CO), confers protective effects on atherosclerosis. These benefits include anti-inflammatory, anti-oxidant, inhibiting foam cell formation, regulating ion channels and enhancing cell adhesion and endothelial functions[9]. Sodium hydrosulfide (NaHS) is the most conventional H_2S donor, however, it only provides a transient H_2S stimulus. In contrast, GYY4137, a water-soluble compound first synthesized by Philip K. Moore et al., acts as a slow-releasing H_2S donor that enables sustained release of H_2S[10]. Previous study has demonstrated GYY4137 exhibited anti-atherosclerosis by preventing atherosclerotic plaque formation and destabilization in apolipoprotein E (-/-) mice[11]. However, the specific impact of GYY4137 on macrophages-derived foam cells and the mechanism-potentially involving autophagy-remain unclear.

This study aims to explore the effect and underlying mechanism of the hydrogen sulfide donor GYY4137 in ox-LDL-induced macrophage foam cell formation, which is used to mimic atherosclerosis in *vitro*.

2. Materials and methods

2.1 Cell Culture and Differentiation

Human acute monocytic leukemia cells (THP-1) were purchased from the Chinese Academy of Sciences and cultured in RPMI1640 medium (invitrogen) containing 10% fetal bovine serum. The cells were maintained in routine culture at 37 ℃ with 5% CO_2 incubator. Cell density reached 80% confluence when the cells were passaged. THP-1 monocyte was differentiated to THP-1 macrophage (THP-M) through 100 ng/mL phorbol ester (PMA, Sigma) for 48 hours. Then, THP-M were incubated with ox-LDL to induce THP-1 macrophage differentiated foam cell (THP-F).

2.2 Cell Counting Kit-8 (CCK-8)

Cells were seeded in 96-well plates. After THP-1 cells were differentiated into THP-M macrophages, they were starved for 12 h. The cells were then treated with ox-LDL at various concentrations (0, 40, 80, 120, 160, and 200 μg/mL) for 24 h. Blank wells containing only culture medium were included, and each concentration was tested in triplicate. After the treatment, the original medium was removed, and 100 μL

of diluted CCK-8 solution (Dojindo) was added to each well. The plates were incubated at 37°C in a 5% CO_2 atmosphere for 30 min. The absorbance of each well was measured at 450 nm using a microplate reader, and the values were recorded.

2.3 TC, Fch and CE content

Total cholesterol (TC) and free cholesterol (Fch) were measured by cholesterol esterase assay following the manufacturer's protocols. Cholesterol standards (5 mmol/L) were serially diluted in absolute ethanol (39-2500 μmol/L) for calibration, with ethanol as a blank. THP-M cells, induced with an optimal ox-LDL concentration for 24 h in 6-well plates, were lysed. Subsequently, 10 μL of blanks, standards, or sample lysates were added in triplicate to a 96-well plate containing 190 μL of freshly prepared working solution. After 20 min incubation at 37°C, absorbance was measured at 550 nm. Sample TC and Fch concentrations were calculated from standard curves. Cholesteryl Ester (CE) = TC-Fch.

2.4 Oil red staining

Cells were cultured in 12-well plates and then were stimulated with the predetermined optimal concentration of ox-LDL to induce foam cell formation. Then, the cells were washed with PBS before being fixed with ORO Fixative for 20 minutes. After fixation, the cells were rinsed with distilled water and then treated with 60% isopropanol for 5 minutes. Then, the cells were stained with a freshly prepared Oil Red O solution (Solarbio) for 15 minutes. The cells were thoroughly washed with distilled water. Nuclei were then counterstained with Mayer's hematoxylin for approximately 1 minute, the cells were washed with water. Finally, cells were dipped in ORO Buffer for 1 minute and then were covered with distilled water for microscopic observation and image acquisition.

2.5 Western-blot

WB was carried out referring to the previous report[4]. After induction with the appropriate concentration of ox-LDL, the cell precipitates of each group were collected and lysed with RIPA Lysis buffer (Beyotime, Shanghai). The total protein concentrations were determined using a BCA assay kit (Beyotime, Shanghai). Each protein sample was added 5 × loading buffer at a ratio of 1:4 and incubated at 95°C for 10 min for denaturation. Equal amounts of proteins were separated by SDS-PAGE (HyClone) and then transferred to PVDF membranes (CST). The membranes were blocked with 5% skimmed milk (Servicebio, Wuhan) for 1 h at 37°C and incubated with the corresponding primary antibody overnight. The primary antibodies included the following: LC3B Rabbit mAb, P62 Rabbit mAb (CST) and GAPDH Rabbit mAb (Abcam). Then the membranes were washed with TBST (Servicebio) and incubated with HRP-conjugated secondary antibody (Goat anti-rabbit IgG, Immunoway, Shanghai) at 37°C for 1 h. The blots were visualized using enhanced chemiluminescence (ECL, Beyotime, Shanghai, China) and quantified by Image J software (National Institutes of Health, USA).

2.6 Statistical Analysis

Statistical significance was calculated through one-way ANOVA, followed by the Tukey's post hoc test among multiple groups using GraphPad Prism software. $P < 0.05$ indicated statistical significance. Data

are displayed as the mean ± standard deviation.

3. Results

3.1 Optimization of ox-LDL concentration for foam cell formation in THP-M

THP-1 monocyte was differentiated to THP-M through 100ng/mL phorbol ester. After induction, most of the cells are spindle-shaped, and some cells extend pseudopodia (Fig. 1A). THP-M were incubated with ox-LDL and the results showed that the activity of THP-M decreased significantly when the ox-LDL concentration was 200μg/mL (Fig. 1B). Then, the ox-LDL concentrations of 0,40,80,120,160 μg/mL were selected for subsequent experiments. To validate foam cell formation, which is characterized by an intracellular CE/TC ratio > 50%, we measured the intracellular levels of TC, Fch, and CE. The results showed a concentration-dependent increase in these lipid components in response to ox-LDL stimulation (Fig. 1C ~ E). The ratio of cholesterol esters to total cholesterol in THP-M cells treated with different concentrations of ox-LDL as shown in Table 1. Internationally recognized definition of foam cells[12]: CE/TC > 50%. Based on the cholesterol esterase assay, an ox-LDL concentration of 160 μg/mL was selected to treat THP-M cells and induce foam cell formation. And then we used Oil Red O staining to validate foam cell formation. As shown in Fig. 1F and G, only a few red-stained lipid droplets were observed in the control group. In contrast, the ox-LDL-treated group showed abundant red lipid droplets aggregated inside the cells, along with some ruptured cells and spilled lipids, consistent with the typical features of foam cells. These findings support the successful establishment of the atherosclerosis cell model.

Table 1 Ratio of cholesterol esters to total cholesterol in THP-M cells treated with different concentrations of ox-LDL (CE/TC) (x±S, n=3)

ox-LDL(μg/mL)	CE/TC (%)
0	20.44±1.04
40	22.40±1.96
80	37.64±5.27
120	48.35±2.77
160	55.74±2.49**

Note: **Compared with 50%, p<0.01.

(A) THP-1 monocyte was differentiated to THP-M; (B) Detection of cell viability of THP-M after induction by ox-LDL; (C ~ E) The contents of TC, Fch and CE in THP-M induced by different concentrations of ox-LDL; (F) Oil Red O staining images of THP-M cells (ox-LDL = 0 μg/mL). (G) Oil Red O staining images of

THP-M cells (ox-LDL = 160 μg/mL) $^{*}p < 0.05$, $^{**}p < 0.01$ vs control group (ox-LDL concentration was 0 μg/mL).

3.2 ox-LDL induces autophagic dysfunction in THP-M

ox-LDL induced THP-M for 24 hours, the ratio of LC3Ⅱ/LC3Ⅰ increased in a dose-dependent manner. When the concentration of ox-LDL was 0-120μg/mL, the expression of p62 protein decreased in a concentration-dependent manner. When the concentration of ox-LDL was 160 μg/mL, the expression of p62 protein in cells increased. These findings indicate that low-to-moderate ox-LDL promotes autophagic flux in THP-M cells, whereas high-dose ox-LDL may induce autophagy initiation but impair late-stage autophagic degradation, leading to p62 accumulation. Then, THP-M cells were treated with Baf-A1 for 24 hours. Compared with the control group, the Baf-A1 group could significantly increase the protein expressions of LC3Ⅱ/LC3Ⅰ and p62 in the cells. Compared with the Baf-A1 + ox-LDL group, the expression of LC3Ⅱ/LC3Ⅰ protein in the Baf-A1 group increased, with a significant difference, while the expression of p62 protein did not change significantly (ns). These findings confirm that Baf-A1 blocks late-stage autophagy flux, leading to LC3Ⅱ and p62 accumulation, and further verify that ox-LDL can induce autophagy initiation even under autophagic degradation inhibition.

(A) THP-1 monocyte was differentiated to THP-M; (B) Detection of proliferation activity of THP-M after induction by ox-LDL; (C ~ E) The contents of TC, Fch and CE in THP-M induced by different concentrations of ox-LDL (F ~ G). $^{*}p < 0.05$, $^{**}p < 0.01$ vs control group (ox-LDL concentration was 0 μg/mL).

3.3 GYY4137 inhibits ox-LDL-induced autophagy in THP-M

Then, we investigated whether GYY4137 could reduce ox-LDL-induced autophagy in THP-M. Firstly, THP-M were treated with GYY4137, and we found that there is no effect of GYY4137 on THP-M when the concentration was range from 50 to 400 μmol/L (Fig. 3A). The WB results showed that compared with the control group, the LC3Ⅱ/LC3Ⅰ ratio and p62 protein level were increased in the foam cell. It indicated that excessive autophagy occurred at this time. Compared with the Ox-LDL group, the LC3Ⅱ/LC3Ⅰ protein level decreased in cells treated with GYY4137 at concentrations ranging from 50 to 400 μmol/L, the p62 protein expression level decreased significantly when the concentration of GYY4137 was in the range of 100 to 400 μmol/L, while GYY4137 at a concentration of 50 μmol/L failed to reduce the p62 protein expression (Fig. 3B **~ D**). It means GYY4137 can inhibit autophagy in the foam cell.
(A) Detection of cell viability of THP-M after induction by GYY4137; (B) Typical Western-blot lanes of LC3II, LC3I and p62. (C) and (D) Statistical analyses of LC3II/LC3I and p62. $^{\#\#}p < 0.01$ vs Control. $^{*}p < 0.05$, $^{**}p < 0.01$ vs Ox-LDL.

4. Discussion

AS is a complex chronic inflammatory disease that underpins the pathogenesis of most cardiovascular diseases (CVDs), including coronary heart disease and myocardial infarction, and remains a leading

cause of global mortality and morbidity[1]. The formation of foam cells, primarily derived from monocyte-derived macrophages that excessively phagocytose ox-LDL, is a critical initiating event in AS progression. This pathological transformation not only promotes lipid accumulation in the arterial wall but also triggers sustained inflammatory responses, accelerating plaque formation and instability[4]. In this study, we established a reliable AS model by differentiating THP-1 monocytes into macrophages (THP-M) using phorbol ester (PMA) and subsequent induction with ox-LDL. Our results confirmed that 160 μg/mL ox-LDL was the optimal concentration for foam cell formation, as evidenced by Oil Red O staining showing massive intracellular lipid droplet accumulation and CE/TC ratio exceeding 50%-a key criterion for defining foam cells[12]. This model effectively mimics the early lipid metabolic disorders in AS, providing a robust platform to explore the protective effects and mechanisms of the hydrogen sulfide (H_2S) donor GYY4137.

Autophagy, a highly conserved intracellular catabolic process, plays a dual role in AS development[5]. Under physiological conditions, autophagy maintains cellular homeostasis by degrading damaged organelles, misfolded proteins, and excess lipids, thereby exerting a protective effect against foam cell formation. However, dysregulated autophagy, particularly impaired autophagic flux, can lead to the accumulation of autophagic substrates and exacerbate cellular stress, promoting AS progression[13]. The conversion of LC3-I to LC3-II and the degradation of p62 are widely used to evaluate autophagic activity and flux. Our study revealed a dose-dependent effect of ox-LDL on autophagy in THP-M cells: low-to-moderate concentrations (0-120 μg/mL) of ox-LDL increased the LC3-II/LC3-I ratio and decreased p62 expression, indicating enhanced autophagic flux that may help clear excess lipids and prevent early foam cell formation. In contrast, at the foam cell-inducing concentration of 160 μg/mL ox-LDL, the LC3-II/LC3-I ratio remained elevated while p62 expression was significantly upregulated, suggesting that high-dose ox-LDL induces autophagy initiation but impairs late-stage autophagic degradation. To further validate this finding, we used Bafilomycin A1 (Baf-A1), a specific inhibitor of late-stage autophagy that blocks autophagosome-lysosome fusion. The results showed that Baf-A1 treatment alone significantly increased LC3-II/LC3-I ratio and p62 expression compared to the control group, confirming its inhibitory effect on autophagic flux. Moreover, compared with the Baf-A1 monotherapy group, the Baf-A1 + ox-LDL co-treatment group exhibited a significantly lower LC3-II/LC3-I ratio but no significant change in p62 expression. This indicates that ox-LDL can still induce autophagy initiation even when autophagic degradation is blocked, while the accumulated p62 in the Baf-A1 group is partially consumed by ox-LDL-induced autophagosome formation, resulting in no significant difference in p62 levels between the two groups. Collectively, these data demonstrate that high-dose ox-LDL triggers autophagic dysfunction in THP-M cells, shifting autophagy from a protective mechanism to a pathological process that contributes to foam cell formation.

H_2S, recognized as the third gas transmitter following NO and CO, has emerged as a promising therapeutic candidate for AS due to its diverse biological activities, including anti-inflammation, antioxidant stress, regulation of lipid metabolism, and protection of cardiovascular disease[14]. Compared with traditional H_2S donors such as sodium hydrosulfide (NaHS), which release H_2S rapidly and transiently, GYY4137 is a water-soluble, slow-releasing H_2S donor that mimics the physiological

continuous release of H_2S, leading to more stable and sustained biological effects. Previous studies have shown that GYY4137 inhibits atherosclerotic plaque formation and destabilization in apolipoprotein E (-/-) mice via regulating the PI3K/Akt and TLR4 signaling pathways[11]. However, its specific effects on ox-LDL-induced macrophage-derived foam cells and the role of autophagy in this process remain unclear. In our study, CCK-8 assay results showed that GYY4137 at concentrations ranging from 50 to 400 μmol/L had no significant cytotoxicity on THP-M cells, confirming its safety. Western blot analysis revealed that compared with the ox-LDL-induced foam cell group, GYY4137 treatment (50–400 μmol/L) significantly reduced the elevated LC3-II/LC3-I ratio, and p62 expression was also significantly decreased at concentrations ≥ 100 μmol/L (while 50 μmol/L GYY4137 had no significant effect on p62 expression). These findings indicate that GYY4137 can inhibit ox-LDL-induced excessive autophagy and restore impaired autophagic flux in foam cells, which may contribute to its protective effect against foam cell formation. Notably, the regulatory effect of GYY4137 on autophagy did not follow a strict dose-dependent pattern: lower concentrations of GYY4137 (50–100 μmol/L) exhibited a more pronounced inhibitory effect on autophagosome accumulation, while higher concentrations (200–400 μmol/L) showed no further enhancement of this effect.

Several limitations of this study should be acknowledged. First, this is an in *vitro* study using a macrophage foam cell model, which only simulates the early stages of AS. Second, the specific molecular mechanisms by which GYY4137 regulates autophagic flux remain unclear. Future studies should focus on key signaling pathways involved in autophagy to identify the precise targets of GYY4137. Third, our study only explored the effects of GYY4137 on macrophage-derived foam cells; its effects on other cell types involved in AS, such as vascular endothelial cells and smooth muscle cells, require further investigation.

5. Conclusion

In conclusion, our study demonstrates that high-dose ox-LDL induces foam cell formation in THP-M cells by triggering autophagic dysfunction, characterized by impaired autophagic flux. The H_2S donor GYY4137 exhibits a protective effect against ox-LDL-induced foam cell formation by inhibiting excessive autophagy and restoring autophagic flux balance, without significant cytotoxicity. These findings highlight the potential of GYY4137 as a novel therapeutic agent for AS and provide new insights into the interplay between H_2S signaling, autophagy, and foam cell biology. Future research focusing on the molecular pathways underlying GYY4137-mediated autophagic regulation and its in *vivo* efficacy will further promote the clinical translation of GYY4137 for the prevention and treatment of cardiovascular diseases.

Declarations

Ethics approval and consent to participate

Not applicable.

Consent for publication

All authors have approved the final manuscript for publication.

Availability of data and materials

The datasets analyzed during the current study are available from the corresponding author on reasonable request.

Competing interests

The authors declare that they have no competing interests.

Funding

Research and Development Program Projects of North Sichuan Medical College CBY25-QDA13.

Authors' contributions

Luo Lijun, Yu Chunlei and Zhou Chunyang; Conception and design: Zhou Chunyang and Yang Chunyang; Acquisition of data: Luo Lijun, Huang Rong and Dong Qiuhong; Statistics analysis: Luo Lijun and Dong Qiuhong; Manuscript writing: Luo Lijun; Critical revision: Zhou Chunyang.

Acknowledgements

Not applicable.

References

1. Roth GA, et al. Global Burden of Cardiovascular Diseases and Risk Factors, 1990–2019: Update From the GBD 2019 Study. J Am Coll Cardiol. 2020;76(25):2982–3021.
2. Chong B, et al. Global burden of cardiovascular diseases: projections from 2025 to 2050. Eur J Prev Cardiol. 2025;32(11):1001–15.
3. Libby P. The changing landscape of atherosclerosis. Nature. 2021;592(7855):524–33.
4. Ajoolabady A, et al. Inflammation in atherosclerosis: pathophysiology and mechanisms. Cell Death Dis. 2024;15(11):817.
5. Choi AM, Ryter SW, Levine B. Autophagy in human health and disease. N Engl J Med. 2013;368(7):651–62.
6. Heckmann BL, Green DR. LC3-associated phagocytosis at a glance. J Cell Sci, 2019. 132(5).
7. Huang X, et al. S-acylation of p62 promotes p62 droplet recruitment into autophagosomes in mammalian autophagy. Mol Cell. 2023;83(19):3485–e350111.
8. Wang Y, et al. LncRNA LUCAT1 offers protection against human coronary artery endothelial cellular oxidative stress injury through modulating hsa-miR-6776-5p/LRRC25 axis and activating autophagy

flux. J Transl Med. 2024;22(1):1171.
9. Liu HT, et al. EndMT: Potential Target of H(2)S against Atherosclerosis. Curr Med Chem. 2021;28(18):3666–80.
10. Li L, et al. Characterization of a novel, water-soluble hydrogen sulfide-releasing molecule (GYY4137): new insights into the biology of hydrogen sulfide. Circulation. 2008;117(18):2351–60.
11. Zheng Y, et al. GYY4137 exhibits anti-atherosclerosis effect in apolipoprotein E (-/-) mice via PI3K/Akt and TLR4 signalling. Clin Exp Pharmacol Physiol. 2020;47(7):1231–9.
12. Fogelman AM, et al. Malondialdehyde alteration of low density lipoproteins leads to cholesteryl ester accumulation in human monocyte-macrophages. Proc Natl Acad Sci U S A. 1980;77(4):2214–8.
13. Gatica D, et al. Molecular mechanisms of autophagy in the cardiovascular system. Circ Res. 2015;116(3):456–67.
14. Liang R, et al. Hydrogen sulfide revisited: a stealthy ally in the unseen war against cardiovascular disease. Biochem Pharmacol. 2026;244:117577.

Figures

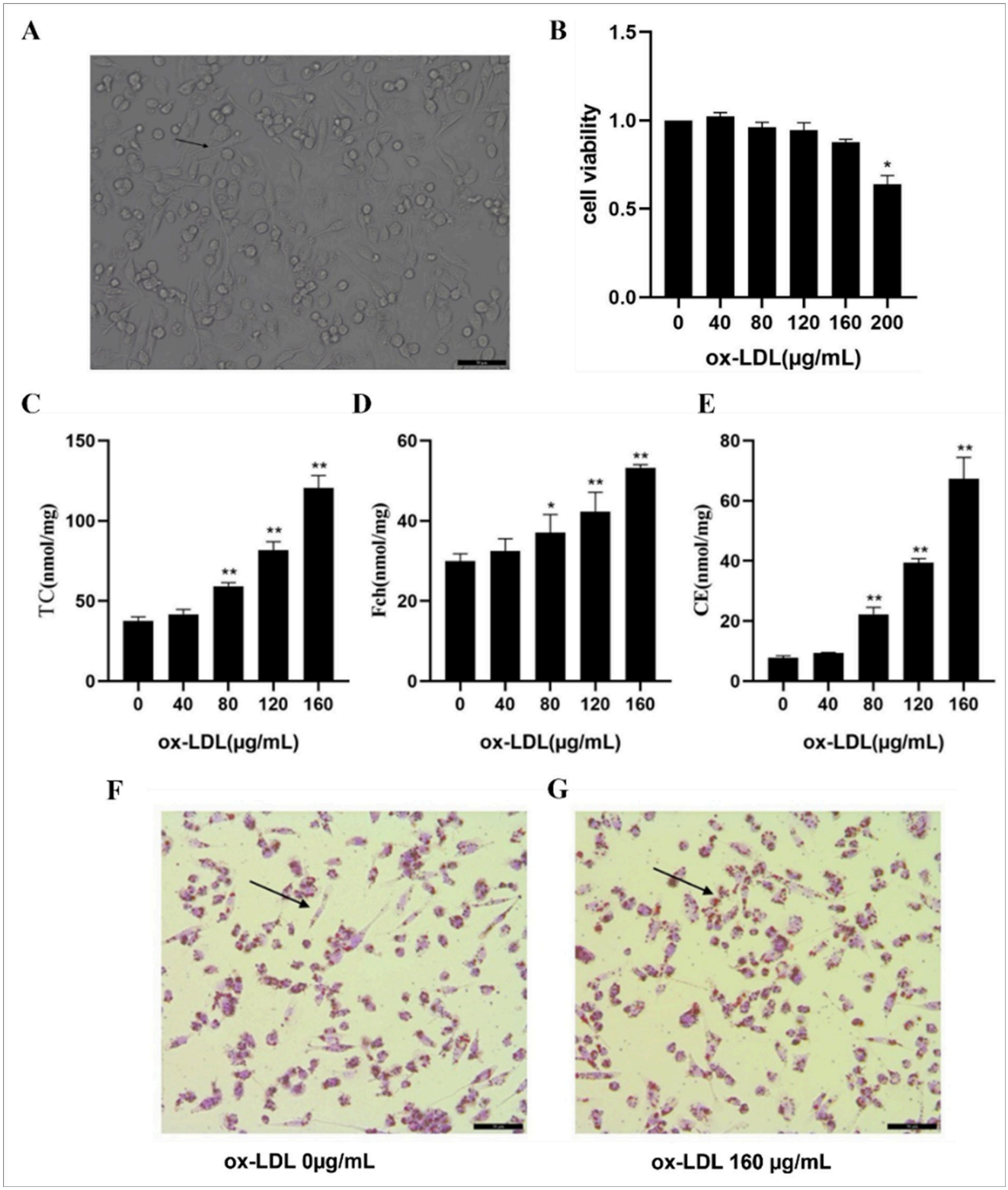


Figure 1

Optimization of ox-LDL Concentration for foam cell formation

(A) THP-1 monocyte was differentiated to THP-M; (B) Detection of cell viability of THP-M after induction by ox-LDL; (C~E) The contents of TC, Fch and CE in THP-M induced by different concentrations of ox-LDL; (F) Oil Red O staining images of THP-M cells (ox-LDL = 0 μg/mL). (G) Oil Red O staining images of

THP-M cells (ox-LDL = 160 μg/mL) $^{*}p<0.05$, $^{**}p<0.01$ vs control group (ox-LDL concentration was 0 μg/mL).

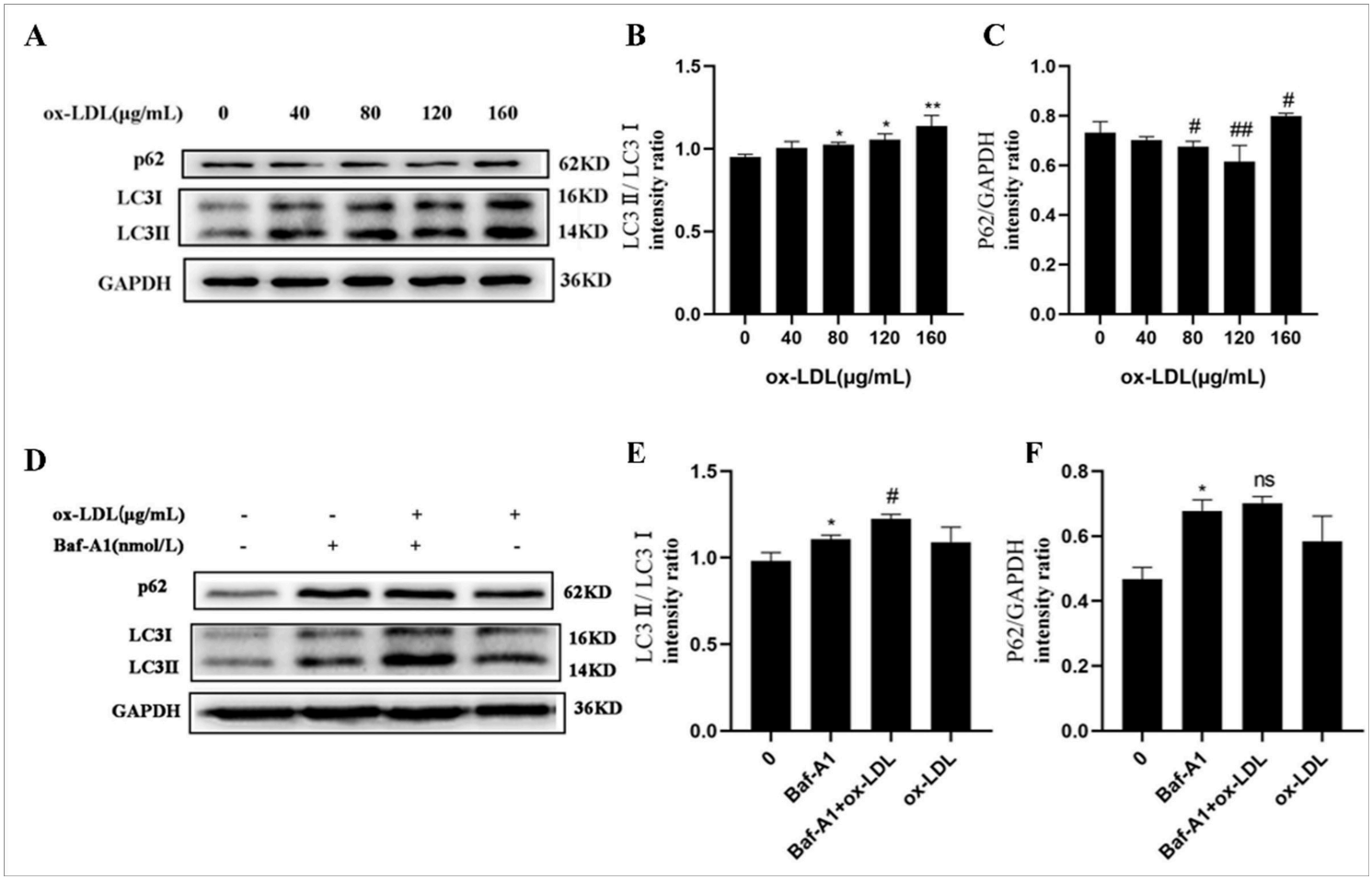


Figure 2

ox-LDL induces autophagic dysfunction in THP-M

(A) THP-1 monocyte was differentiated to THP-M; (B) Detection of proliferation activity of THP-M after induction by ox-LDL; (C~E) The contents of TC, Fch and CE in THP-M induced by different concentrations of ox-LDL (F~G). $^{*}p<0.05$, $^{**}p<0.01$ vs control group (ox-LDL concentration was 0 μg/mL).

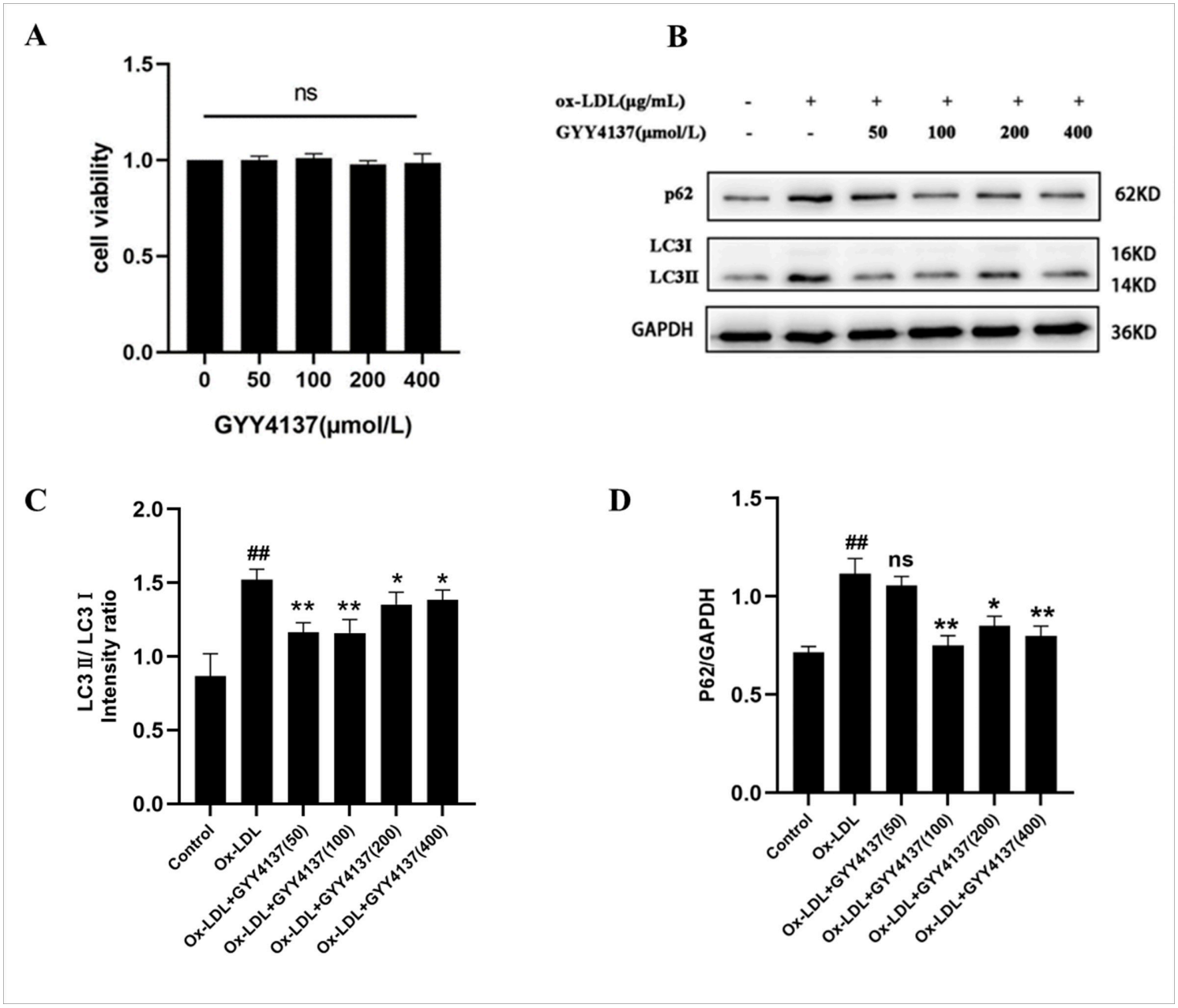


Figure 3

GYY4137 inhibits ox-LDL-induced autophagy in THP-M

(A) Detection of cell viability of THP-M after induction by GYY4137; (B) Typical Western-blot lanes of LC3II, LC3I and p62. (C) and (D) Statistical analyses of LC3II/LC3I and p62. $^{\#\#}p<0.01$ vs Control. $^{*}p<0.05$, $^{**}p<0.01$ vs Ox-LDL.